Deep Mining 2024 – P Andrieux & D Cumming-Potvin (eds)

doi:10.36487/ACG_repo/2465_75

# Empirical and numerical assessment of two extended stopes for dilution estimation in an underground mine

**Adrian I Santos Chauca [a,*], Shahé Shnorhokian [a], Mustafa Kumral [a]**

[a] *Department of Mining and Materials Engineering, McGill University, Canada*

## Abstract

*Over the decades, several empirical and analytical approaches have been developed to assess the stability of underground excavations. For stope design, the stability graph method is commonly used for preliminary sizing assessments. The method has been modified by multiple authors over time using extensive databases to adjust the three factors and boundary limits for the stability zones. Based on field observations, the adjustments were made to improve the qualitative representation of rock mass stability and associated risks. Moreover, different applications such as the dilution graph have been developed based on the stability graph method. The overbreak prediction for open stope footwalls and hanging walls can be quantified with this graph.*

*Numerical modelling is another important tool in rock engineering, commonly utilised in conducting complex analyses in mining. The model consists of numerous elements or zones that discretise the rock mass, requiring initial calibration to predict future results. In the stability graph method, the estimation of induced stress for the stability Factor A purely depends on numerical analysis techniques.*

*In the present study, an assessment is developed for the stability of two extended stopes that were extracted in an underground mine. The stope designs were evaluated using the stability graph method and two versions of the dilution graph. Advanced 3D models were constructed for determining Factor A and for assessing the stability of stope surfaces based on a numerical approach. Finally, a comparison was made between the empirical results of the stability graph method and dilution graph, the numerical models, and actual field observations and cavity monitoring survey (CMS) measurements after the extraction of each stope at the mine.*

**Keywords:** *ore dilution, stability graph method, 3D modelling, extended stopes*

## 1 Introduction

For underground excavation design, the science of rock engineering has developed several geotechnical tools throughout the years to improve rock mass interpretation, predict potential instability conditions, and inhibit rock failure during mining activities. Due to the variability of sizing for excavations, wider openings are expected to impact more on rock mass stability than smaller ones. For instance, the influence of stopes on induced stresses and strain propagations are key parameters that rock engineers must evaluate to ensure mine worker safety and to maximise ore extraction. The effects of exceeding the maximum critical stable dimensions can be severe, especially when considering the high costs of developing stopes. Instability conditions around stope surfaces may result in significant expenses for ground rehabilitation, production delays, mining equipment loss, ore reserve loss, and (in the worst-case scenario) mine worker injuries or fatalities (Potvin & Hadjigeorgiou 2001). Therefore, the importance of stope stability has become an essential assessment not only for determining adequate ground control strategies for the safety of mine workers and mining assets, but also for inhibiting economic losses.

* Corresponding author. Email address: adrian.santos@mail.mcgill.ca

In general, the variability of three key parameters affects the stope stability:

1. rock mass environment around the stope
2. rock mass properties
3. and induced stresses.

Regarding rock mass conditions, depth and topography represent the weight of overlying strata and elevation for the ore deposit, respectively, while geologic structures define the discontinuity systems which can include major and minor faults, stratifications, foliation, and joints. Most rock failure around openings and pillars has been associated with structurally-controlled mechanisms, which have been commonly observed in loss of confinement scenarios. Compressive failure is another common rock failure mechanism that occurs when the induced stresses produced by mining activities exceeds the uniaxial compressive strength (UCS) of the rock mass. In cases where induced stresses are considerably higher than the rock mass strength and the material is defined by brittle characteristics, a violent phenomenon known as rockburst could occur. Hence, rock properties have a significant influence on failure mechanisms in stope surroundings or walls.

Two main approaches have been developed for stope stability assessment:

1. empirical
2. analytical.

The stability graph method is the most common rock engineering tool for preliminary stope design that uses the stability number and hydraulic radius (HR). The first version was introduced by Mathews et al. (1981) and has been modified by multiple authors based on extensive databases from field observations, internal documentation, and published literature to adjust the main three Factors (A, B and C) and stability thresholds. Since the method provides a qualitative stability assessment, Clark & Pakalnis (1997) introduced an empirical dilution graph to quantify the slough volume of stope walls. Capes (2009) developed an extensive database of case studies to update the empirical dilution thresholds. On the other hand, the application of advanced numerical modelling as a rock engineering tool has enhanced the interpretation of rock mass behaviour. Calibrated two and three-dimensional simulations of stopes (combined with underground openings, lithologies, and geological structures) can provide realistic environments for evaluating possible rock mass instability such as compressive or tensile failure, and strain propagation. Numerical models are required for the estimation of Factor A for the stability graph in any case.

Using the approaches mentioned previously, this paper presents case studies of stability assessments for two extended stopes. Unlike a typical stope of 30 m in height, an extended stope is a new proposal based on merging the typical and half-height stope designs into a single one; reducing costs in rock support and development preparation, as well as in operational steps for ore extraction. The current study presents the results of this approach, explaining the limitations of empirical methods and the complexities of numerical modelling as rock engineering tools for the evaluation of wide excavations.

# 2 Mining and geotechnical overview

## 2.1 Site description

Several underground mining methods have been developed and successfully executed at different operations to obtain the most efficient ore extraction, to ensure the safety of all mine personnel, and to provide a sustainable life of mine. Based on wide and complex volcanogenic massive sulphide ore deposit geometry, economic trade-off assessment, and rock mass classification, the current underground case study mine in South America has implemented the transverse sublevel open stoping mining method with pillars. This mining method is shown schematically below in Figure 1.

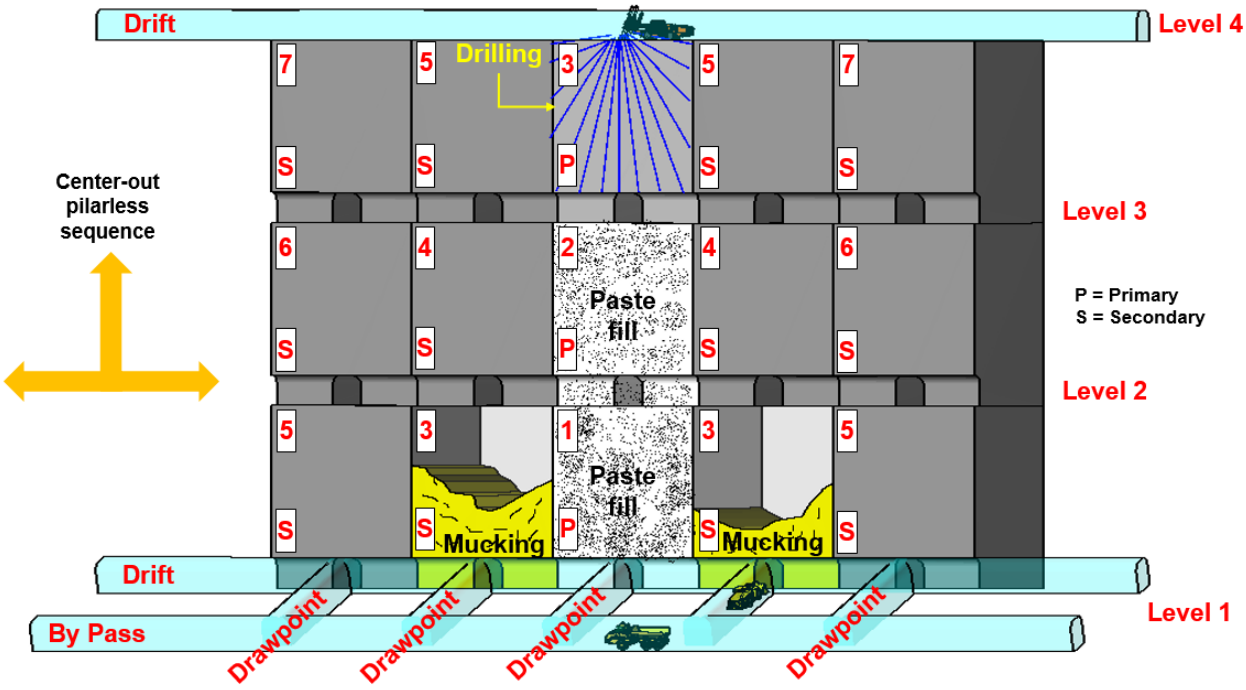


**Figure 1 Transverse sublevel open stoping schematic long section**

The underground operation starts with mining the primary stopes generally following a pyramidal centre-out (bottom up) sequence. This is to avoid high induced stresses at the centre of the deposit, which can make ore recovery difficult. After extraction from the primary stopes is completed, these are backfilled with paste and once it is completely cured (i.e. the material reaches the appropriate strength parameters), the secondary stopes are considered for production. Operationally, primary stopes are those that are not exposed to any backfill wall, while secondary stopes are exposed with a minimum of one backfill wall.

Each stope is composed of two linear development levels:

1. overcut (crown)
2. undercut (drawpoint).

At the overcut level, reinforcement systems such as shotcrete, bolts, cable bolting, or mesh are installed (depending on rock mass characterisation) to strengthen the rock mass and mitigate the instability conditions resulting from the wide span of the stope. At the undercut level, different rock support systems are installed for the drawpoint excavations to ensure uninterrupted ore mucking. Typically, the undercut and overcut levels are separated by 30 m, which represents the standard height of a stope.

Having followed the transverse sublevel open stoping method for many years, the current underground operation is focused mostly on secondary stopes among different orebodies; some of which are located at the deposit boundary limits. Due to their irregular and complex shapes combined with recent geological ore reclassification, different and challenging stope designs have been considered (including heavy reinforcement systems) to accomplish ore extraction.

Two main designs that have been implemented with good results are:

1. Half-height stope, which is shorter than the standard dimension of 30 m. A competent sill pillar in the crown (or roof wall) is provided, which is sufficiently stable during the extraction. This design is suitable for fair to good rock mass characterisation (i.e. rock mass rating [RMR] above 41).
2. Linear development-breasting with upward blastholes towards stopes without shoulders. When the stope shoulders are potentially unstable or collapsed due to either geotechnical or operational reasons, a linear development-breasting preparation is required to build a new

undercut level for a typical or half-height stope using upward blastholes. Operationally, no rock support can be installed in these cases.

Even though these mining steps are widely used at the underground operation and provide positive results, some technical reports indicate that a complex procedure (based on extra rock support systems and linear developments) at specific stopes not only increases the cost but can also slow down the mining rate by adding more operational hours. Therefore, additional geotechnical research has been conducted for stopes with extended height dimensions at the boundary limits.

## 2.2 Extended stope design

The new proposal for this case is based on merging the typical and half-height stope designs into one extended vertical stope. Instead of investing in rock support at the overcut level for stope 'A' and developing a linear breasting for the stope 'B' unique undercut level, both stopes are unified into an extended vertical one (Figure 2) that can be extracted in fewer steps, ensuring the same tonnage recovery and controlling any stability risks.

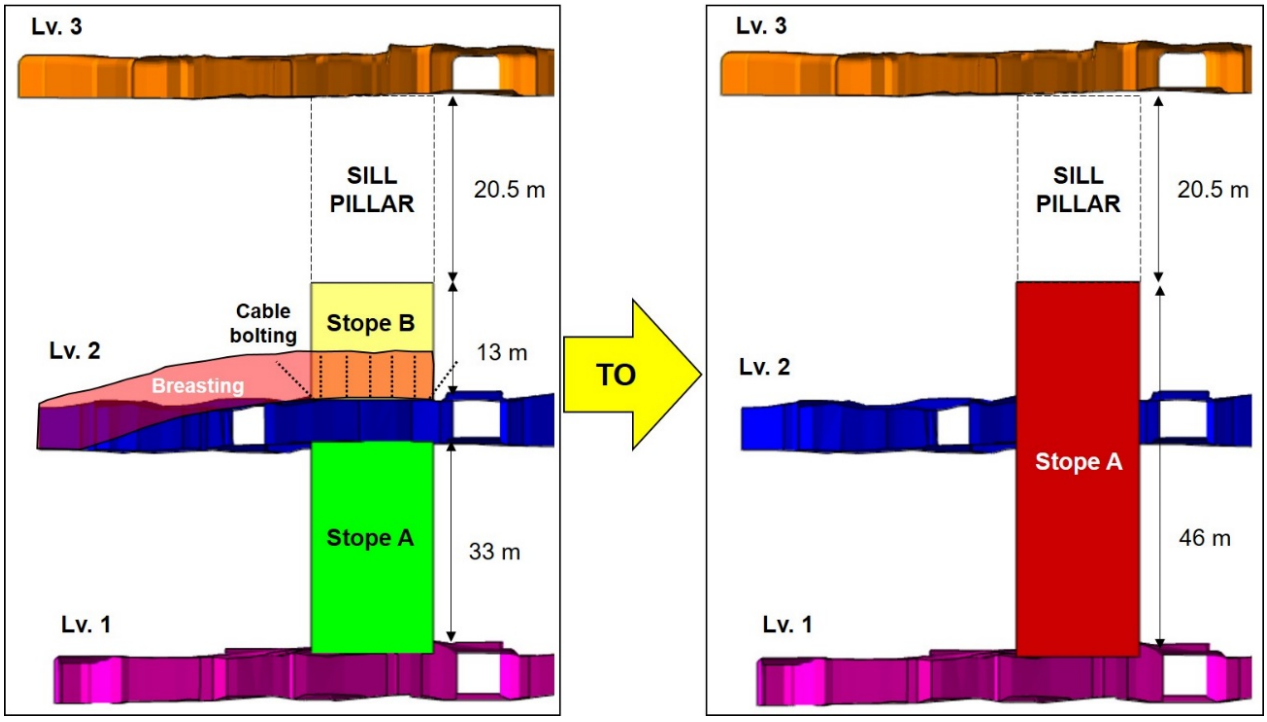


**Figure 2 Typical mining design and new proposal design (extended vertical stope)**

### *2.2.1 Case studies*

The current case studies are for two extended stopes (stope 1 and stope 2) having the dimensions indicated in Figure 3. Since stope 1 has two faces exposed to paste fill, only the remaining two faces (the northwest [NW] and the southwest [SW]) and the back wall (crown) will be considered for stability and dilution assessment. Stope 2 has one face exposed to paste fill, and therefore the north (N), south (S), east (E), and the back wall are evaluated for stability and potential dilution. Based on the new proposal design, both stopes remain unsupported. While analytical and numerical methods were used to assess stability in this study, the main objective was to evaluate potential savings and to optimise stope designs.

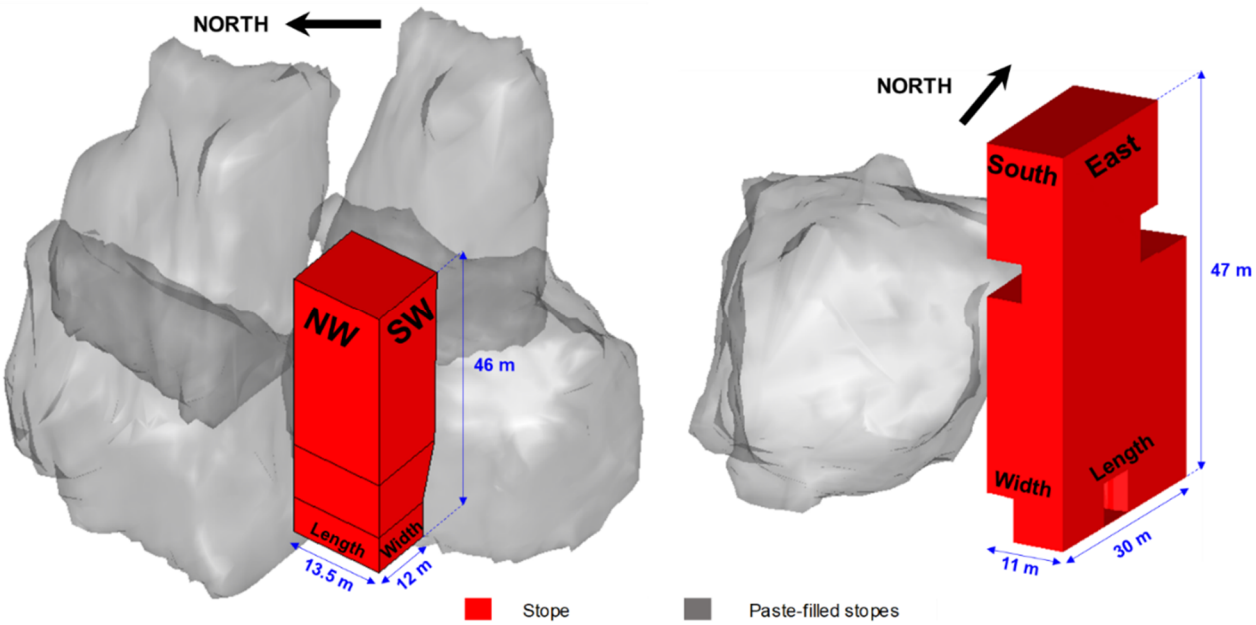


(a) (b)

**Figure 3 Dimensions and mining conditions of (a) Extended stope 1; (b) Extended stope 2**

### *2.2.2 Rock mass characterisation*

The extended stopes are located predominantly in favourable rock mass zones (i.e. fair rock mass rating of 48 and rock quality designation of 60%, on average). Due to the complex geological shape, some of the stope walls were situated in the ore lithology, which has an average uniaxial compressive strength (UCS) of 65 MPa. During the field geotechnical investigations, joint sets parallel to the SW and back walls were found for extended stope 1. Similarly, for extended stope 2, joint sets parallel to the N, E and S walls were observed.

Based on the in situ stress measurements, the orientation for the major and minor horizontal stresses were determined in the north–south and east–west directions, respectively. After conducting several calibration techniques, the horizontal-to-vertical stress ratios were obtained as $K_{N\text{-}S}$ = 1.6 and $K_{E\text{-}W}$ = 1.2.

# 3 Methodology

Both empirical and numerical modelling approaches were used to evaluate stope stability in this study, as explained below.

## 3.1 Empirical approach

### *3.1.1 Stability graph method*

For open stoping design, the stability graph method introduced by Mathews et al. (1981) (and modified by Potvin (1988) and other authors) is the most widely used tool for empirical sizing assessments. The stability number (N') and HR represent the vertical and horizontal axes in the stability graph, respectively. The HR is calculated by dividing the area of a stope wall with its perimeter. N' is calculated through the following formula (Equation 1):

$$N' = Q' \times A \times B \times C \quad (1)$$

In this case, Q' is the modified rock mass classification developed by Potvin (1988) that represents the block size factor and the shear strength of the critical joint, and Factors A, B, and C are measurements based on induced stresses, main structures, and gravity effects (respectively) on each free face. In addition, the

authors redefined the stability zones to 'stable' and 'caved', with a narrow transition zone in between. Nickson (1992) conducted a more extensive statistical assessment based on discriminant and linear regression analyses to refine the 'stable with support' zone.

Using the stability graph method for the extended stope designs for this study, their dimensions were plotted on two chart versions to evaluate their utility and limitations (Figure 4), as this was the design procedure used at the mine. It should be noted that the Potvin (1988) and Nickson (1992) charts are different in that the latter comprises data from stopes with support elements.

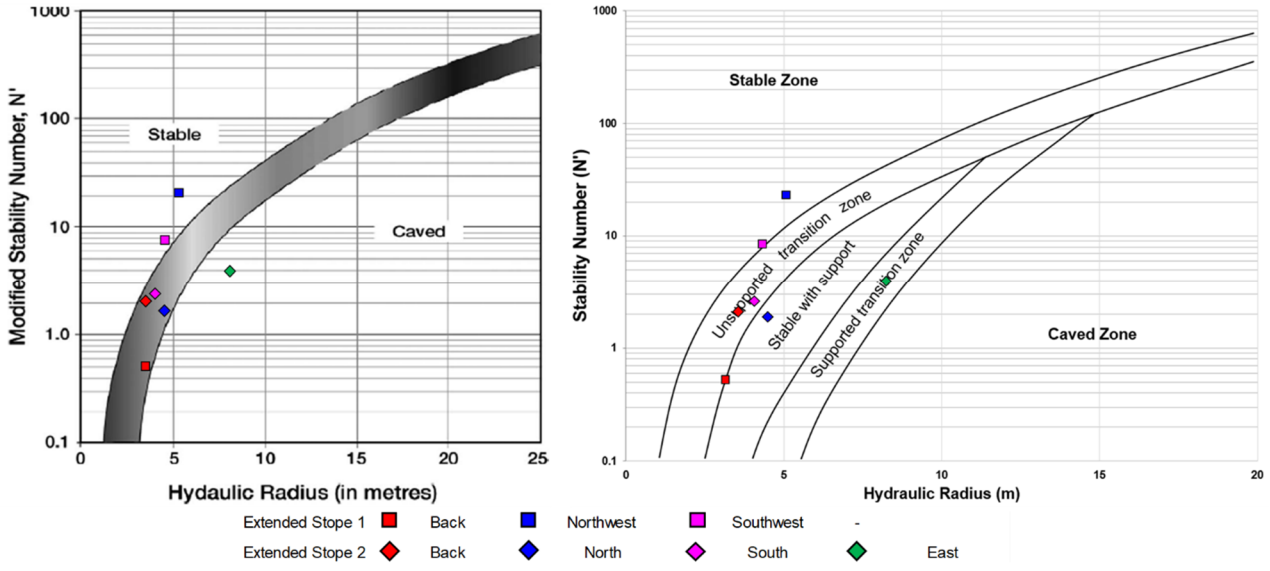


**Figure 4 (a) Modified stability graph (Potvin 1988); (b) Modified stability graph (Nickson 1992) showing a refined zone 'stable with support'**

### *3.1.2 Dilution graph*

Researchers such as Stewart & Forsyth (1995), Hutchinson & Diederichs (1996), and Potvin & Hadjigeorgiou (2001), provide some general insights about dilution on stope walls based on the stability graph zones. Results of ore dilution and recovery for a specific open stope are related to the mining technique and design. Considering that these two indicators are interdependent, an optimal design maximises recovery and minimises dilution (Clark & Pakalnis 1997).

Suorineni (2012) reports that for open stoping size dimensioning, the original stability graph of Mathews et al. (1981) is useful for providing a qualitative assessment of whether a given stope surface is stable, unstable, or caving. Despite this capability, he concludes, the presence of potential dilution cannot be determined with precision by this graph. Quantitative dilution levels are important because a specific mine can use this information to determine their appropriate levels during stope sizing design. Indeed, the type of ore extracted, and mining methods applied, will impact acceptable dilution levels, which vary from mine to mine. Unlike the results from the original stability graph, Clark & Pakalnis (1997) introduced the equivalent linear of overbreak or sloughing (ELOS) concept for quantitative dilution values. They emphasise the implementation of the cavity monitoring system (CMS) which has significantly improved the actual surveying of open stopes with high precision. However, only unplanned dilution can be quantified with CMS stope surveys. The authors utilised an extensive database of 47 open stopes – which was correlated with the modified stability graph – to develop an empirical method for estimating unplanned dilution.

For the empirical stability factor, Clark & Pakalnis (1997) proposed considerations such as stress Factor A set at 1 (stope walls are in low-stress or tensile states), joint orientation Factor B set at 0.3 (critical joint parallel to the stope wall), and gravity Factor C set at 8 for all footwalls and (8–6 cos[dip]) for hanging walls (dip as the stope hanging wall inclination). The authors also underlined a better definition of Factor C for footwalls.

The ELOS Factor was introduced as a measurement of the unplanned dilution for a specific stope wall, which allows the quantification of the potential amount of wall slough during stope design, as given in Equation 2.

$$ELOS = \frac{Volume\ of\ slough\ from\ stope\ surface}{Stope\ height \times wall\ strke\ length} \quad (2)$$

The ELOS design chart developed by Clark & Pakalnis (1997) indicates the following areas for unplanned dilution: blast damage only (ELOS < 0.5 m), minor sloughing (ELOS = 0.5–1.0 m), moderate sloughing (ELOS = 1.0–2.0 m), and severe sloughing or possible wall collapse (ELOS > 2 m). Capes (2009) collected a large database of 255 case studies to update the dilution graph from Clark & Pakalnis (1997) and increased the dataset inside a zone of interest delimited by stability numbers between 0.2 and 10, and hydraulic radii between 2 and 10 m. Similarly, he assumed the same stability factors from Clark & Pakalnis (1997). The logistic regression methodology was utilised to develop the probability lines for ELOS < 0.5 m, < 1 m, < 2 m, and < 4 m showing the maximum number of correct predictions for each of the 255 case studies above and below each ELOS line. For correct classification, these results coincide with 80% of cases with ELOS > 4 m plotting below the ELOS < 4 m line, and 77% of cases with ELOS < 4 m plotting above the ELOS < 4 m line. The stability number and HR of each extended stope wall were plotted on the dilution graph of Clark & Pakalnis (1997) and Capes (2009) to evaluate their usage and limitations, as shown in Figure 5.

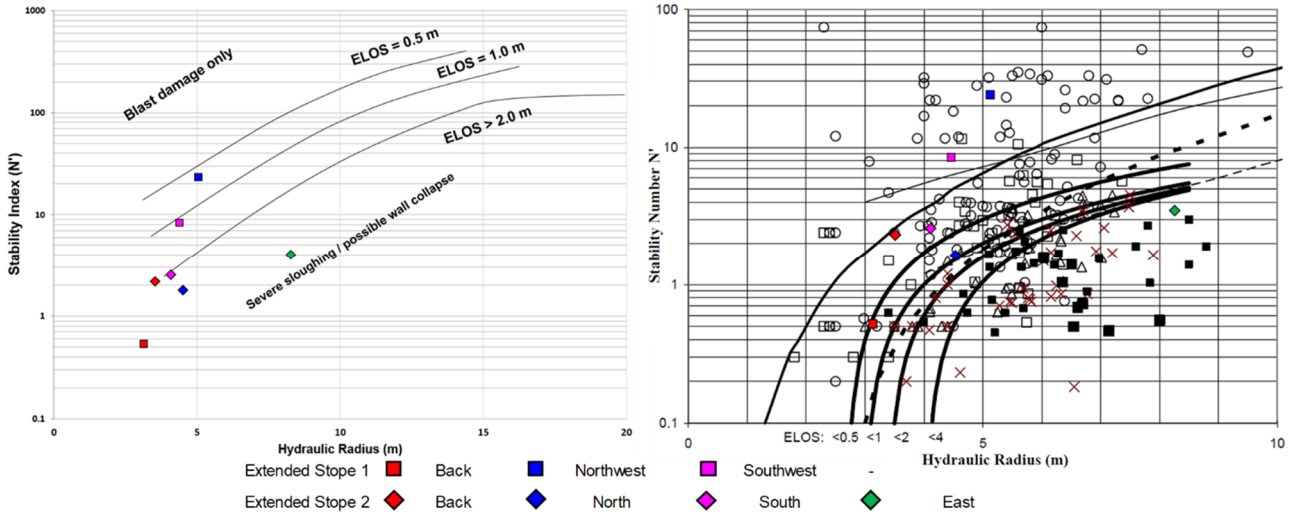


**Figure 5 (a) Empirical unplanned dilution graph (Clark & Pakalnis 1997); (b) Dilution graph based on highest percentage correct classification: 255 case database (Capes 2009)**

Limitations in the empirical design such as the set values for the stability Factors A, B, and C, and the limited size of the database were underlined by Clark & Pakalnis (1997), while Capes & Milne (2008) indicated the challenges in quantifying rock mass properties. All authors state that to improve the interpretation of each stope wall stability, external factors with potential influence were required, such as stope geometry, rock mass classification, undercutting of stope walls, drilling, blasting, stope support, and stand-up time.

## 3.2 Numerical approach

Two advanced numerical analyses were conducted using StopeX and FLAC3D to assess the stability of stope walls and back for each extended stope, and to compare the results with the empirical evaluations using the stability graph method and dilution graph. StopeX is an add-on tool to FLAC3D that uses the FISH code for model construction and adopts an improved unified constitutive model (IUCM) for elasto-plastic strain-softening simulation, in addition to comprising a traditional linear elastic option. The IUCM is deemed to provide an accurate and comprehensive representation of rock mass behaviour, particularly in a stress-strain relationship (Vakili 2016). For this study and based on a comparison between linear elastic and IUCM simulations, the former was adopted to generate enhanced stresses for maximum compressional and

shear instability. Most of the lithological units were included in each of the extended stope models to make them as representative as possible of the actual field conditions at the mine.

For extended stope 1, the extents of the FLAC3D model along the east–west, north–south, and elevation coordinates along the depth reach 1,250 m, 1,250 m, and 1,120 m, respectively. Similarly, for extended stope 2, model dimensions along the east–west, north–south, and elevation coordinates along the depth attain 800 m, 750 m, and 1,050 m, respectively. The rock mass properties that the model input parameters were derived from are presented in Table 1. The GSI was calculated using the RMR conversion (Hoek et al. 1995) in Equation 3:

$$GSI = RMR - 5 \quad (3)$$

The models were calibrated based on stress measurements at 450 m depth given the following magnitudes: $\sigma_H$ (maximum horizontal stress) at 19.1 MPa in a N–S orientation ($K_H$ = 1.6), $\sigma_h$ (minimum horizontal stress) at 14.3 MPa in an E–W orientation ($K_h$ = 1.2), and $\sigma_V$ at 11.9 MPa in the vertical direction. Traditional roller boundary conditions were set by StopeX for the sides and bottom and the top was left free, with initialisation used for generating the in situ stresses.

**Table 1 Rock properties**

| Model | Rock type | GSI | Young's modulus $E_i$ (MPa) | Density (t/m$^3$) | Poisson's ratio |
|---|---|---|---|---|---|
| **Extended stope 1** | Ore | 46 | 28,160 | 4.5 | 0.235 |
| | Host rock | 42 | 33,207 | 2.7 | 0.24 |
| | Dyke | 58 | 48,013 | 2.8 | 0.273 |
| | Backfill | - | 50 | 2.4 | 0.25 |
| **Extended stope 2** | Ore | 45 | 34,360 | 4.5 | 0.20 |
| | Host rock | 42 | 32,840 | 2.8 | 0.27 |
| | Backfill | - | 50 | 2.7 | 0.25 |

For the model stages in both scenarios, the developments were excavated first. Then for the first model (extended stope 1) a mining sequence based on stopes extraction from 2018 to 2021, inclusive, was implemented on an annual basis. For the second model (extended stope 2) a detailed mining sequence for each stope extraction was developed. Finally the extended stope was mined in the last stage for both models.

In this study, the FLAC3D models were run in linear elastic mode to provide a more conservative analysis of potential instability. Since high stresses were not expected due to the relatively shallow depths of the orebodies, tensile stress is the criterion that could be expected to be active in providing instability on the walls and in the back. As such, and due to variable rock mass properties, $\sigma_3$ values above zero were assessed and plotted in FLAC3D to compare with the stability and ELOS assessments from the empirical analyses.

Numerical modelling outputs such as major principal stress, minor principal stress and maximum shear stress were plotted in two- and three-dimensional figures to enhance the interpretation. For the current stope assessments, the major principal stress and maximum shear stress contours were plotted as 65 and 25 MPa, respectively, combined with the plane base level in the model to evaluate potential high-stress zones around the stopes (Figures 6 and 7). The 65 MPa contours were used for comparison with the average UCS of the orebody and some compressional failure zones are found (Figure 6), but they are not located on the stope walls. For shear stresses, the 25 MPa contours represent the equivalent value for a brittle share ratio (BSR) (the two being related through the differential stress) of 0.7 for a major potential of strainbursting. No isosurfaces of 25 MPa can be observed in Figure 7, which means no rockbursting failure is expected to take place.

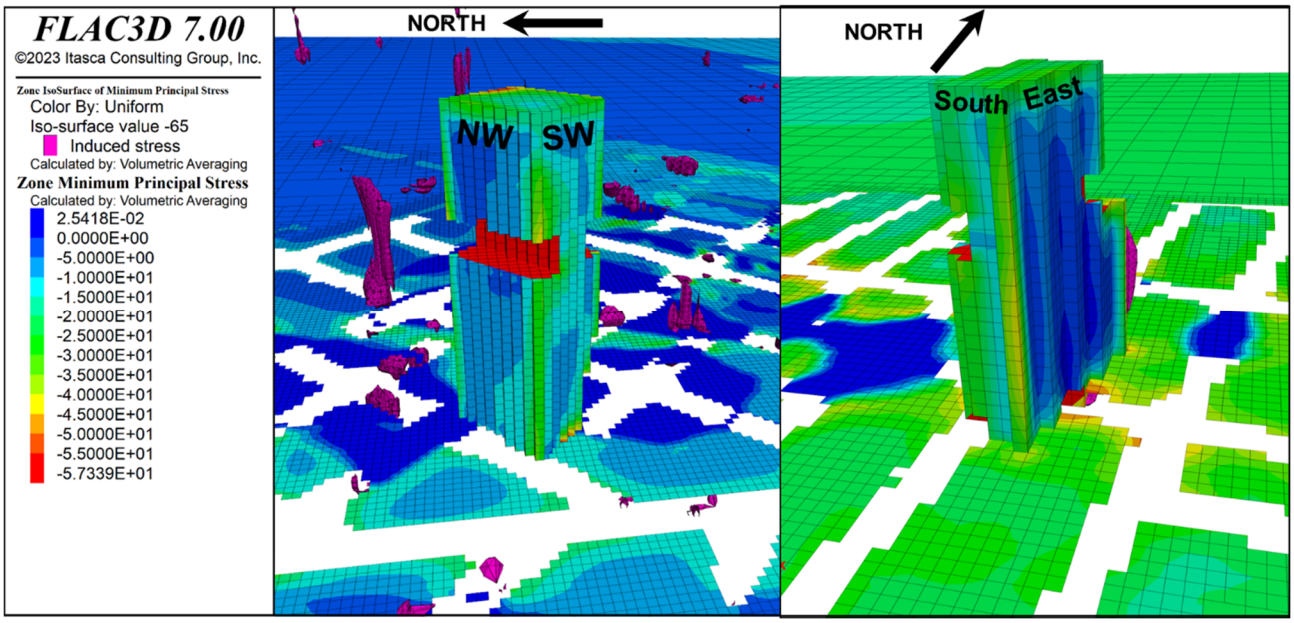


(a) (b)

**Figure 6 (a) Major principal stresses contours for the extended stope 1 after extraction and before backfilling (back, north–west, and south–west walls); (b) Major principal stress contours for the extended stope 2 (back, north, east and south walls) after extraction and before backfilling**

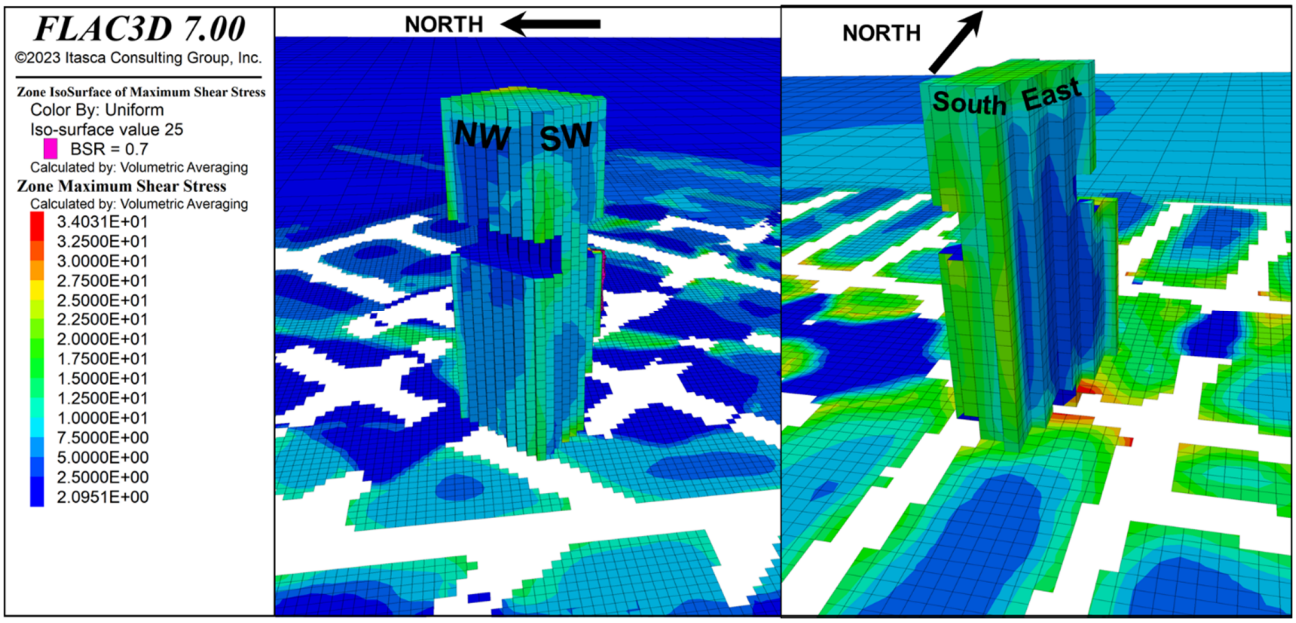


(a) (b)

**Figure 7 (a) Major shear stresses contours for the extended stope 1 after extraction and before backfilling (back, north–west, and south–west walls); (b) Major principal stresses contours for the extended stope 2 after extraction and before backfilling (back, north, east and south walls)**

Similarly, minor principal stress contours were plotted as 0 MPa (tensile zone) isosurfaces in the two models combined with the plane base level to evaluate relatively low-stress and tensile instability around the stopes (Figure 8). Both extended stopes present instability zones based on the tensile isosurfaces. In the case of stope 1, major failure zones are observed in the NW wall compared to the SW one, while the back wall reports minor failure. In the case of stope 2, the most critical failure is observed on the east wall compared with the south and north wall.

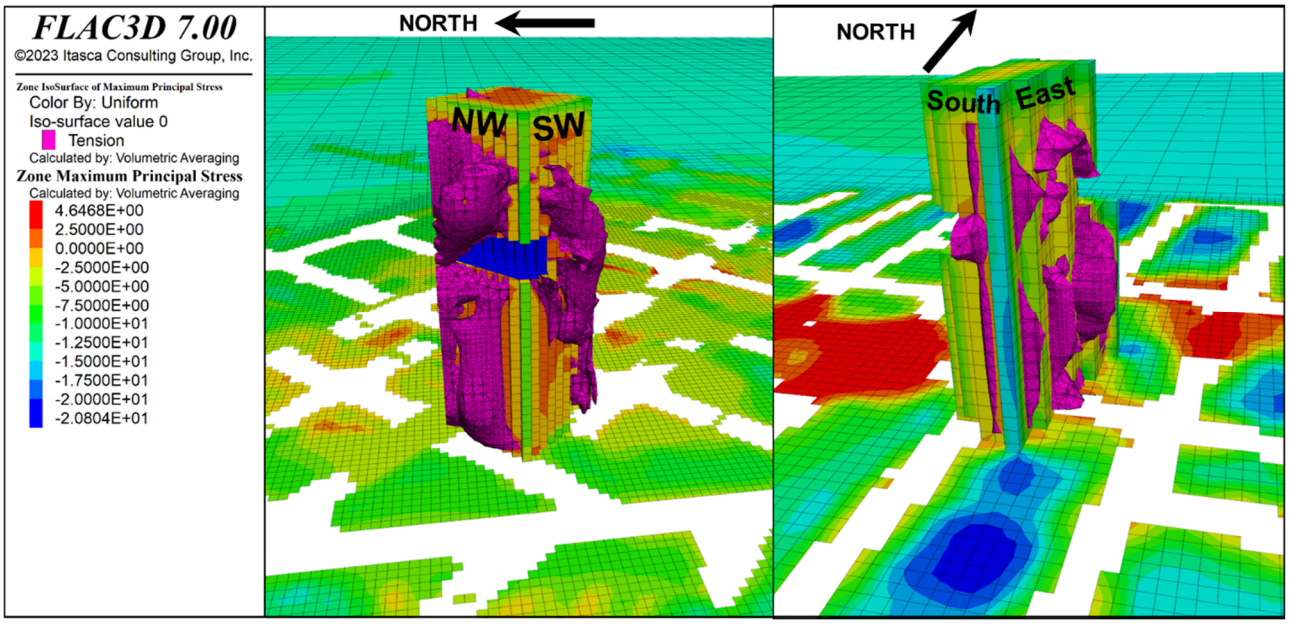


(a) (b)

**Figure 8 (a) Minor principal stresses contours for the extended stope 1 after extraction and before backfilling (back, north–west, and south–west walls); (b) Minor principal stresses contours for the extended stope 2 after extraction and before backfilling (back, north, east and south walls)**

## 3.3 Field observations

The extended stopes not only required complex technical design and operational procedures but also constant CMS scans to control any instability condition in the rock mass surrounding the wide excavation. Once the extraction was completed, a final CMS scan was conducted to measure the void spaces in the two cases (Figure 9). This information is reported as ELOS (m) and volume ($m^3$) in Table 2 to compare with the unplanned dilution values obtained from the empirical and numerical modelling approaches, respectively.

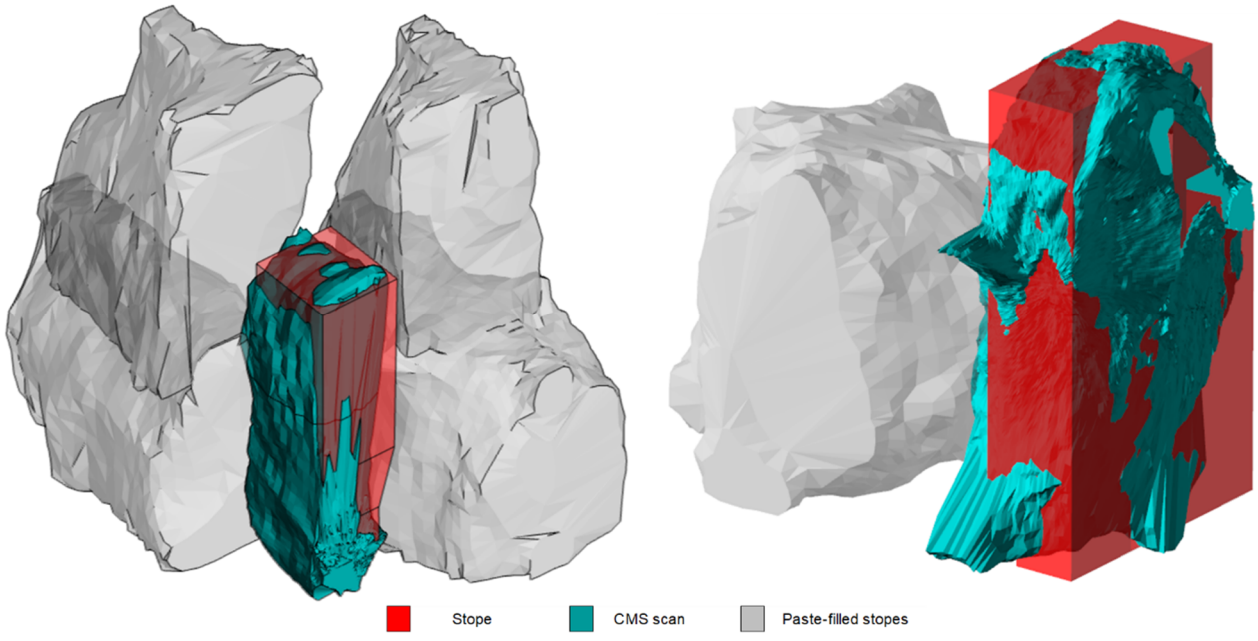


(a) (b)

**Figure 9 (a) Final cavity monitoring system (CMS) scan of the extended stope 1; (b) Final CMS scan of the extended stope 2**

**Table 2 Unplanned dilution (volume [m³] and equivalent linear of overbreak or sloughing [ELOS] [m]) from cavity monitoring system scan**

| Model | Stope wall | Volume (m³) | Area (m²) | ELOS (m) |
|---|---|---|---|---|
| **Extended stope 1** | Back | 35 | 162 | 0.22 |
| | NW | 389 | 555 | 0.70 |
| | SW | 65 | 455 | 0.14 |
| **Extended stope 2** | Back | 89 | 233 | 0.38 |
| | N | 150 | 527 | 0.29 |
| | E | 1,473 | 1,261 | 1.17 |
| | S | 172 | 469 | 0.37 |

# 4 Results and discussions

After plotting the results for each stope wall on the two stability charts, different results were obtained. Similarly, the ELOS values for the empirical unplanned dilution were plotted using the two charts mentioned above and varying results were obtained. The values from both the stability and ELOS results are presented in Table 3.

**Table 3 Stability and equivalent linear of overbreak or sloughing (ELOS) results from different charts**

| Model | Stope wall | Potvin (1988) | Nickson (1992) | Clark & Pakalnis (1997) | Capes (2009) |
|---|---|---|---|---|---|
| **Extended stope 1** | Back | Transition zone | Unsupported transition zone | > 2 m | 0.5–1.0 m |
| | NW | Stable | Stable | 0.5–1.0 m | Stable |
| | SW | Stable | Stable | 1.0–2.0 m | Stable |
| **Extended stope 2** | Back | Transition zone | Unsupported transition zone | > 2 m | < 0.5 m |
| | N | Transition zone | Stable with support | > 2 m | 0.5–1.0 m |
| | E | Caved | Supported transition zone | > 2 m | > 4 m |
| | S | Transition zone | Unsupported transition zone | > 2 m | 0.5–1.0 m |

Although the stability graphs modified by Potvin (1988) and Nickson (1992) are different since the second author gathered a larger database, adding more stability zones and support elements, the results obtained by these charts are generally similar. In addition, these two charts were the ones used for design purposes at the mine, and they are adopted in this study to provide a basis for comparison with the numerical modelling output.

In the first extended stope, the side walls (NW and SW) remain ‘stable’, but the back wall is in the ‘transition zone’ between the ‘stable’ and ‘caved’ zones (Potvin 1988), and between the ‘stable’ and ‘stable with support’ zones (Nickson 1992). Therefore, instability conditions on the back wall could occur during

mucking activities in the stope, and both charts provide comparable assessments with the additional information with respect to support in the second one.

Outcomes for the second extended stope based on Potvin's (1988) chart indicate that the east wall is expected to cave, but the remaining stope walls (back, north, and south) are in the 'transition zone' between the 'stable' and 'caved' zones. Using Nickson's (1992) chart, the back and south walls are in the 'transition zone' between 'stable' and 'stable with support', the north wall remains 'stable with support', and the east wall is in the 'transition zone' between 'stable with support' and 'caved'. Hence, instability conditions are expected to occur from each wall of the second extended stope with major rock mass failure from the east wall. While varying results were obtained from the two stability graph method charts, the ones based on Nickson's (1992) version were more comparable to the factual data obtained from the mine. This could be due to several factors such as the empirical database for each chart being different, the use of support in the second one, and the deterministic nature of both approaches.

Regarding ore dilution, the ELOS results from Clark & Pakalnis' chart (1997) indicate unplanned dilution during the production stage of both stopes, when each stope is at its maximum excavated span before backfilling is implemented. This is despite the stability charts predicting stable zones for the stope walls of the first extended stope. On the other hand, the ELOS estimation from Capes' chart (2009) indicates different results. For the first extended stope, the NW and SW walls would remain stable, and dilution ($0.5 < ELOS < 1.0$ m) is expected to occur from the back wall. Alternative ELOS outcomes were also obtained for the second extended stope; less than 0.5 m for the back wall, between 0.5 and 1.0 m for the north and south walls, and more than 4 m for the east wall. These latter unplanned dilution values match the results from the empirical stability graph from Nickson (1992), despite the fact that no support was used in either of the extended stopes at the mine.

Using the FLAC3D model, three instability criteria for the different stope walls were applied:

1. compressive failure ($\sigma_1 > UCS$)
2. low-confinement and tensile failure ($\sigma_3 < 0$ MPa)
3. BSR (represented through the maximum shear stress) for major potential of strainbursting.

It should be stated here that in FLAC3D, minimum principal stresses represent $\sigma_1$ and maximum principal stresses represent $\sigma_3$ due to the convention used by the code. Firstly, potential failure zones produced by high induced stress were assessed using the minimum principal stress ($\sigma_1$) magnitudes in the pillars. Given the average UCS for the ore as 65 MPa, the numerical model indicates that no high-stress conditions were observed around the extended stopes at their relatively shallow depths. Thus, no compressive failure is expected even though rock mass fracturing would most likely commence at the $\sigma_1$ values observed there. Secondly, tensile failure zones caused by confinement loss on the stope walls were evaluated using the maximum principal stress ($\sigma_3$) magnitudes below 0 MPa (pure tension) and tensile failure contours were observed around the stope walls. Major instability conditions were found in the NW and east walls of the first and second extended stopes, respectively. Finally, using the UCS value of 70 MPa for the conversion of a BSR value above 0.7 as indicative of strainbursting potential, its equivalent maximum shear stress ($(\sigma_1-\sigma_3)/2$) greater than 25 MPa were plotted. Based on the different contours obtained, no major strainbursting conditions were detected around the stope walls.

In general, no high-stress conditions were observed around the stope walls. However, tensile failure has been found in the NW and east walls of the first and second extended stopes, respectively, which represent imminent rockfall and can be quantified as potential unplanned dilution. Although the ELOS methodology provides either a linear representation of overbreak or volume, the numerical modelling exhibits the actual contours and shapes of the dilution blocks. In a future study, the authors plan to use volumetric analysis to conduct a quantitative assessment of dilution from these two extended stopes.

# 5 Conclusion

Since the first introduction of the stability graph method, the approach has been modified by multiple authors based on extensive databases to adjust the three factors and resulting curves. Since the reliability of the empirical method largely depends on the quality and the size of the database, a specific site stability graph could increase the level of precision for each stope assessment.

Even though several limitations were found during the development of the empirical dilution graphs, Capes' chart (2008) provides acceptable preliminary results for the dilution estimation of each stope wall from both extended stopes in this study. Factors that influence the accuracy and applications of the design method are represented by difficulties of rock mass properties determination and external factors (mining) that influence stope stability.

According to the results from the FLAC3D model, no critical unstable conditions referring to low-confinement and potential tensile failure, that could produce imminent rock falling, were observed through contours of the back walls in each extended stope. While minor and major rock failure contours were obtained from both extended stope side walls. Specifically, in the FLAC3D model, the highest tensile failure contours were found in the NW and east walls of the first and second extended stopes, respectively, indicating high dilution levels which match with the CMS scan. The accuracy of these dilution observations could not be predicted or quantified with the empirical approach using either stability or dilution graphs. On the other hand, the numerical results did not match dilution results from other walls in the extended stopes, which could be due to the use of linear elastic modelling in this initial study or deterministic input parameters for the rock mass properties.

The new proposal of using extended stopes at the case study mine is an outcome of favourable field investigations plus rock engineering. The design provides high quantity savings for rock support, rehabilitation, and breasting linear development compared with a typical stope design. It will be very interesting to conduct a quantitative volumetric assessment of dilution from the FLAC3D models and compare it with the CMS scan, and the actual volume of rock failure in situ. Once model results are validated with the field data, it could provide a very powerful numerical tool for estimating dilution in underground mines.

# Acknowledgement

The authors would like to acknowledge Itasca for the provision of FLAC3D licenses through the Itasca Educational Partnership (IEP) Teaching Program to the Department of Mining and Materials Engineering at McGill University. The authors would also like to acknowledge Cavroc for the free provision of an educational license of StopeX.

# References

Capes, G & Milne, D 2008, 'A compilation of dilution graph data for open stope hangingwall design', in Y Potvin, J Carter, A Dyskin & R Jeffrey (eds), *SHIRMS 2008: Proceedings of the First Southern Hemisphere International Rock Mechanics Symposium*, Australian Centre for Geomechanics, Perth, pp. 149–162, https://doi.org/10.36487/ACG_repo/808_19

Capes, G 2009, *Open Stope Hangingwall Design Based on General and Detailed Data Collection in Rock Masses With Unfavourable Hangingwall Conditions*, PhD thesis, University of Saskatchewan, Saskatoon.

Clark, L & Pakalnis, R 1997, 'An empirical design approach for estimating unplanned dilution from open stope hangingwalls and footwalls', *Proceedings of the 99th annual general meeting*, Canadian Institute of Mining, Metallurgy and Petroleum, Vancouver.

Hoek, E, Kaiser, PK & Bawden, WF 1995, *Support of underground excavations in hard rock*, AA Balkema Publishers, Brookfields.

Hutchinson, DJ & Diederichs, MS 1996, *Cablebolting in Underground Mines*, BiTech Publishers Ltd, Richmond.

Mathews, KE, Hoek, E, Wyllie, DC & Stewart, SBV 1981, *Prediction of Stable Excavation Spans for Mining at Depths Below 1000m in Hard Rock*, CANMET Report DSS Serial No. OSQ80-00081, DSS File No. 17SQ. 23440-0-9020, Canada Department of Energy Mines and Resources, Ottawa.

Nickson, SD 1992, *Cable Support Guidelines For Underground Hard Rock Mine Operations*, MASc thesis, University of British Columbia, Vancouver.

Potvin, Y 1988, *Empirical Open Stope Design in Canada*, PhD thesis, University of British Columbia, Vancouver.

Potvin, Y & Hadjigeorgiou, J 2001, 'The stability graph method for open stope design', in Hustrulid & Bullock (eds), *Underground Mining Methods*, Society of Mining Engineers, pp. 513–520.

Stewart, SBV & Forsyth, WW 1995, 'The Mathew's method for open stope design', *CIM bulleting*, vol. 88, pp. 45–53.

Suorineni, FT 2012, 'A critical review of the stability graph method for open stope design', *MassMin 2012: 6th International Conference & Exhibition on Mass Mining,* Canadian Institute of Mining, Metallurgy and Petroleum, Sudbury, https://doi.org/10.13140/2.1.4353.0561

Vakili, A 2016, 'An improved unified constitutive model for rock material and guidelines for its application in numerical modelling', *Computers and Geotechnics*, vol. 80, pp. 261–282, https://doi.org/10.1016/j.compgeo.2016.08.020